THE ASTROPHYSICAL JOURNAL, 270:288–299, 1983 July 1

MAGNETIC ROTATION OF THE SOLAR PHOTOSPHERE

HERSCHEL B. SNODGRASS
Mount Wilson and Las Campanas Observatories of the Carnegie Institution of Washington
Received 1982 October 15; accepted 1982 December 9

ABSTRACT

The rotation of magnetic features in the solar photosphere is determined by cross-correlating Mount Wilson magnetograms from observations made over successive days. On this short time scale, the change in field features does not overwhelm their rotational displacement, and, except at the poles, the motion of the correlation peaks is readily followed to determine rotation as a function of latitude. The time period covered is from 1967 January 1 to 1982 May 29, and separate correlations are performed for each of 34 zones of latitude covering the solar disk. To reduce the noise level, sets of corresponding correlations are averaged and rotation is inferred from the displacement of the averaged correlation maximum. This is shown to be an appropriate and powerful technique for smoothing the data, which is indispensable near the poles where the original signal-to-noise ratio is marginal.

The variance of the determined means ranges from $\sim 0.1\%$ (~ 2 m s^{-1}) at low latitudes to $\sim 1.1\%$ (~ 10 m s^{-1}) near the poles, and to this accuracy there is no significant variation with time nor dependence on field strength over the whole $15\frac{1}{2}$ year period. The differential rotation profile rises from agreement with the Mount Wilson Doppler profile near the poles to close agreement with the Newton and Nunn sunspot results in sunspot latitudes, where it is thus roughly 1.5% (~ 30 m s^{-1}) above the Doppler rate. Using a standard functional fit, we find $\omega(\phi) = 2.902 - 0.464 \sin^2 \phi - 0.328 \sin^4 \phi$ microrad s^{-1}, where ϕ is the solar latitude. In addition there is a slight dimple (~ 8 m s^{-1}) at the equator, similar to that seen in the Doppler curve.

Subject headings: Sun: magnetic fields — Sun: rotation

I. INTRODUCTION

Magnetograph observations (Babcock 1953) made at the 150 foot (46 m) tower telescope at Mount Wilson have been fully digitized since late 1966 (Howard 1974*a*, 1976*a*). Data accumulated on a daily basis since that time include Zeeman splittings and line shifts for the spectral line λ5250.2 of Fe I measured for 11,000, and after 1973 when the scanning aperture was reduced from 17.5 arcsec^2 to 12.5 arcsec^2, 23,000 square patches covering the solar disk. A part of each day's data reduction is the spectroscopic determination of photospheric plasma rotation. The details, results, and analysis of this program are reported in Howard and Harvey (1970), Howard and Yoshimura (1976), Howard, Boyden, and LaBonte (1980), LaBonte and Howard (1981*a*), Howard *et al.* (1983), and LaBonte, Howard, and Gilman (1981). This program has recently been highlighted by the discovery of torsional oscillations with an 11 year period (Howard and LaBonte 1980; LaBonte and Howard 1981*b*, 1983).

The daily magnetogram, or map of longitudinal solar photospheric magnetic field strengths, is a second major product of the data reduction; this paper uses the magnetograms to get an independent determination of solar rotation. Detailed studies of solar magnetic fields, based on these data, can be found in Howard and Stenflo (1972), Howard and Edberg (1973), Howard (1974*b*, *c*, *d*, 1976*b*, 1977), Altschuler *et al.* (1974), and Howard and LaBonte (1981). That the magnetic fields, examined from day to day, show differential rotation has long been known from synoptic charts (Bumba and Howard 1965), but previous quantitative studies of magnetic rotation are almost all based on auto-correlations (Wilcox and Howard 1970; Wilcox *et al.* 1970; Stenflo 1974, 1977). Although these studies, which wait for patterns to recur after complete rotations, also find differential rotation, it is less pronounced than that seen either from tracing visible photospheric features or from measuring Doppler shifts, and in one study (Wilcox *et al.* 1970), it is found to change dramatically as the correlation time lag is increased to include several rotations.

The differences among rotation profiles from Doppler measurements, from tracing visible features, and from magnetic autocorrelations pose interesting questions. Evidence that the Doppler rate is less than the sunspot and plage rates (Howard 1978*b*) suggests that weaker and nonmagnetic regions may rotate more slowly, but the suggestion that the still higher and flatter magnetic autocorrelation profile (Stenflo 1974) is further evidence for this possibility seems unlikely since sunspots and plages already are the regions of strongest field. The problem with autocorrelations is the time scale: except for strong sunspots and plages where mangetograms tend to saturate anyway, magnetic features characteristically do not last more than a few days. After a full rotation, the correlation is quite feeble and the scatter

in results correspondingly large. This condition thwarted a recent attempt (LaBonte, unpublished) to fit autocorrelation results with functions analogous to those used to fit Doppler results (Howard, Boyden, and LaBonte 1980), and even in the most careful projects (Stenflo 1974, 1977) where sunspot fields are put in by hand and autocorrelations are averaged over long periods, it is not clear what aspects of the magnetic field the autocorrelations are picking up.

It may be, as suggested by Howard (1978*a*, *b*), that what is being seen is the rotation of a larger, deeply rooted magnetic structure, which though of low amplitude compared with the photospheric field features, outlasts them. If so, perhaps also the photospheric features arise through interaction of this deeper structure with the photospheric plasma; magnetic rotation might thus be an important tool for linking what is seen in the photosphere with what is happening deeper within the Sun.

A study of magnetic rotation at high latitudes by Howard (1978*a*, *b*) followed the motion of features on *successive* days' magnetograms, thus reducing the time scale; large scatter was again a problem, but here it was due to the weakness of the polar features plus the convergence of polar meridians in relation to the size of the scanning aperture. In the present study we employ cross-correlation to examine the short-term rotation of fields over the whole surface of the Sun: magnetograms, divided into latitude strips, are cross-correlated at increments of 1, 2, 3, and 4 successive days. The period covered is $15\frac{1}{2}$ years from 1967 January 1 to 1982 May 29, for which the digitized magnetograms are available. Strictly speaking, this is therefore a study of *magnetogram* rotation, focusing on the smoothed, ambient fields $\lesssim 100$ guass that are emphasized by the Mount Wilson angular resolution.

II. METHOD

As part of the reduction procedure at Mount Wilson, the raw data are binned in a "coarse array," which is a map of the solar disk onto a square grid of 34×34 latitudes and longitudes. In the present study, the binned fields are Lagrange interpolated onto a grid with equal longitude intervals and then cross-correlated separately along each of the 34 strips of latitude. The longitude interval chosen is 3°, slightly less than the 3°.4 width of the coarse array bins at central meridian, and the total longitudinal data window is fixed at $\pm 36°$, which represents a compromise between having sufficient points for a reasonable calculation and minimizing errors due to limb effects, bin projection, and rotation of the magnetic field vectors, for which we see only the line-of-sight component. We thus start with 24 bins at zero lag, and, as the Sun rotates, the number is reduced until by the fourth day only ~ 7 bins remain near the correlation maximum. Also by the fourth day, the bins actually compared come from near the edges of the window, where the original array grid is considerably coarser than the interpolated grid and the fields compared are rotated by at least 45°; hence 4 days represents the outer limit for which the procedure will work.

Correlating is done using the Pearson cross-correlation (Dodes and Greitzer 1964) where the means are extracted at each lag. Ideally, excepting times when the data are not present, for each day and latitude strip, four cross-correlation curves are computed whose maxima successively trace the strip's magnetic rotation over the next 4 days. Though all indications, e.g., synoptic charts, are that on this time scale the correlations should be strong and dominated by the rotation of photospheric field patterns, the calculated curves still contain a high level of noise which is relatively worse for the higher day lags and toward the poles and clearly stems from the short lifetimes of field features. Consequently, the task of finding and fitting of the "correct" maxima ranges from problematic at low and mid latitudes to impossible in polar regions where the field strengths are barely above instrumental noise to begin with. However, as illustrated in Figure 1, the noise rapidly dwindles when correlation curves are averaged over a set of corresponding day-pairs: the sharp maxima which remain clearly trace the rotation. The positions of these maxima are determined by fitting the curves: as is shown in the Appendix, use of the three-point parabolic fit in conjunction with averaging the correlations yields a sophisticated smoothing of the data wherein spurious values are weeded out while those that cluster around the average are weighted in proportion to the sharpness of their correlation peaks.

In all, for the $15\frac{1}{2}$ year period from 1967 January 1 to 1982 May 29, the available data permit calculation for roughly from 2600 day-pairs for 1 day lags to 2000 day-pairs for 4 day lags. A problem remaining in averaging the correlations before fitting them is the varying times of day of the observations (e.g., a magnetogram taken late sees the Sun rotated further); for the averaging procedure to work, the time intervals must all be identical. This problem is solved by appropriately moving the interpolation grid, which makes the procedure iterative since an estimate of the rotation must be used to do this. Convergence is immediate: while the iteration reduces scatter, it does not significantly alter mean values.

Calculations include three separate passes through the correlated data: a "yearly" pass, in which correlation curves are averaged over entire years before being fitted, a "monthly" pass where the correlations are averaged over 28 day periods (close to the Carrington rotation period of 27.275 days), and a "daily" pass where the individual unaveraged peaks are fitted wherever they lie. Overall time-averaged rates calculated from each pass agree well within their respective error limits, and of course scatter in the daily results is quite large—at mid latitudes it increases with day lag, and at the poles it is consistently overwhelming. The daily polar results appear completely random, but they begin to settle down in the monthly pass and, as will be seen in the next section, are well determined in the yearly pass.

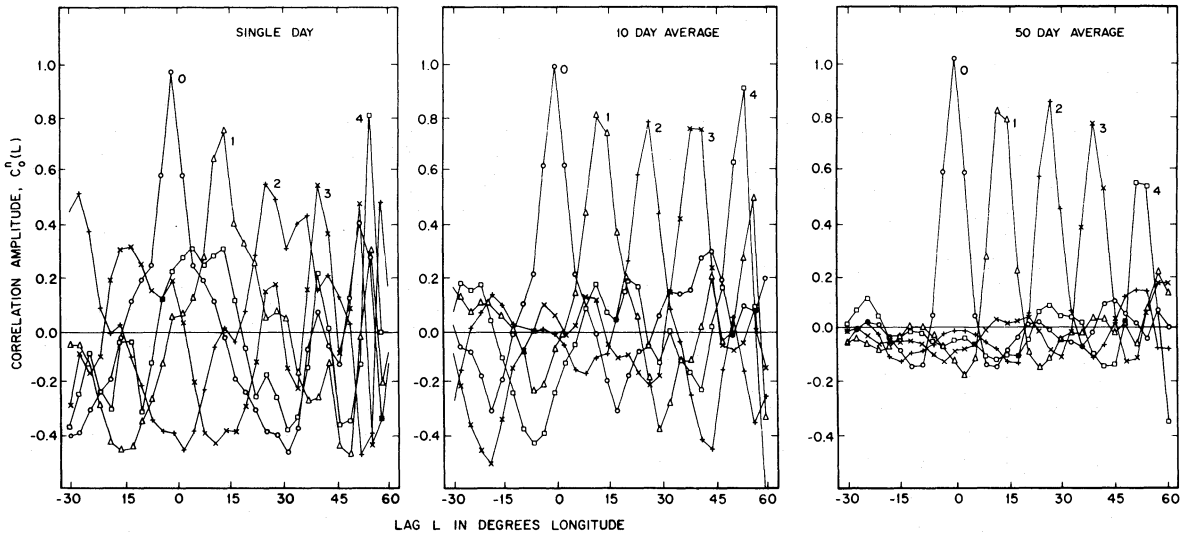

FIG. 1.—Illustration of the effect of averaging correlations. The numbers beside each peak indicate the day lag, or separation in days between the observations that are correlated, autocorrelation being denoted by 0. These are typical mid-latitude results, the "single day" curves represent an unaveraged set of correlation calculations based on a set of 24 3° bins, the lag increments thus being 3°. The 10 day and 50 day sets of curves are averages of such single day calculations over periods of 10 and 50 days respectively.

III. RESULTS

Except near the poles, the scatter in the monthly and the scatter yearly results are comparable; it is thus preferable to concentrate on the monthly results on the possibility that short-term rate variations may be found. Table 1 displays the averages of the monthly (28 day) results over the whole $15\frac{1}{2}$ year period. The $\omega_l(i)$ are rotation rates in microrad s^{-1}, where l is the latitude index and i the day lag, and the $\sigma_l(i)$ are the respective standard deviations of the mean for these quantities. The quantities $\bar{\omega}_l$ and $\bar{\Delta}_l$ are overall averages of averages over the day lags $\bar{\omega}_l$, and of their standard deviations Δ_l. Notice that, at fixed latitude l, the differences among the $\omega_l(i)$ for different day lags i are greater by an order of magnitude than expected from their standard deviations $\sigma_l(i)$; this is also evident in the disparity between σ_l and $\bar{\Delta}_l$. It is seen in § IV that (1) these differences can be accounted for by a systematic error in the correlation calculation and thus most likely do not reflect a solar phenomenon; and (2) in view of this systematic error, the 2 day rate which is consistently greater at mid to low latitudes is to be preferred. Consequently, except near the poles, we focus on the 2 day results.

As expected from the discussion at the end of § II, the rates shown in Table 1 become uncertain at polar latitudes. It is found, referring to Table 2, that for the five most polar latitudes the rates are far better determined from the yearly averaged correlations. Yet, even with the yearly averaging, the random noise overwhelms the criterion for selection of the 2 day lag, so the average over lags $\bar{\omega}_l$ in Table 2 is to be preferred. In Figure 2, these values of $\bar{\omega}_l$ with error bars $\bar{\Delta}_l$ are converted for comparison to degrees per day (synodic) and added to a chart (Howard 1978*a*, Fig. 2) of previous polar rotation studies. They do not support the slower rate inferred by Howard (1978*a*) from a relatively small number of observations; instead, the best agreement is with the Doppler and facular results. It might be added that the results from the unaveraged (daily) correlations would uniformly cover the entire figure; the tightness of our yearly averaged correlations attests to the power of the averaging procedure.

Figure 3 exhibits the magnetic rotation profile averaged over the whole period. The values and errors are $\bar{\omega}_l(2)$ and $\sigma_l(2)$ from Table 1, except for the five most polar latitudes, where they are the $\bar{\omega}_l$ and $\bar{\Delta}_\omega$ from Table 2. For comparison, the Mount Wilson Doppler profile, corrected for fringes and scattered light (LaBonte and Howard 1981*a*; Howard *et al.* 1983) and averaged over the same period, the classical sunspot profile of Newton and Nunn (1951), and the magnetic rotation profile given by Stenflo (1974) are also shown. The present magnetic curve rises from agreement with the Doppler rate near the poles to essentially the Newton and Nunn rate at low latitudes; it thus lies roughly 2% above the Doppler rate near the equator and 1% below the spot rate determined by Ward (1965, 1966).

The equatorial "dimple," well known in the Doppler results (Howard, Boyden, and LaBonte 1980), is also evident, with a magnitude of ~ 8 m s^{-1}, in the magnetic curve of Figure 3. If, as these curves suggest, the magnetic rate is truly faster than the plasma rate, then the dimple in the Doppler curve might reflect the decreased dragging of the plasma by the weaker magnetic fields at the solar equator. But its presence as well in the magnetic curve does not support this suggestion unless there is a tendency also for the magnetic rate to increase with field strength. As mentioned in § I, Stenflo (1974) argued along these lines, taking the comparative flatness

TABLE 1

AVERAGED MAGNETIC DIFFERENTIAL ROTATION FOR 1967 JANUARY 1 TO 1982 MAY 29 BASED ON CORRELATIONS AVERAGED OVER 28 DAY PERIODS

	Latitude	One-Day Lag		Two-Day Lag		Three-Day Lag		Four-Day Lag		Average over Lags		
		$\bar{\omega}_\ell(1)$	$\sigma_\ell(1)$	$\bar{\omega}_\ell(2)$	$\sigma_\ell(2)$	$\bar{\omega}_\ell(3)$	$\sigma_\ell(3)$	$\bar{\omega}_\ell(4)$	$\sigma_\ell(4)$	$\bar{\bar{\omega}}_\ell$	σ_ℓ	$\bar{\Delta}_\ell$
South												
1	-72.8°	2.385	0.061	2.058	0.051	2.346	0.039	2.314	0.034	2.304	0.036	0.262
2	-65.8	2.340	0.038	2.364	0.035	2.294	0.026	2.368	0.024	2.316	0.018	0.163
3	-58.5	2.377	0.025	2.384	0.028	2.294	0.023	2.424	0.021	2.450	0.019	0.128
4	-52.6	2.486	0.017	2.440	0.023	2.462	0.019	2.547	0.017	2.482	0.011	0.113
5	-47.3	2.578	0.016	2.573	0.016	2.524	0.014	2.576	0.013	2.562	0.005	0.071
6	-42.6	2.626	0.012	2.620	0.012	2.627	0.010	2.622	0.015	2.619	0.005	0.051
7	-38.1	2.672	0.011	2.657	0.009	2.668	0.010	2.694	0.011	2.664	0.004	0.037
8	-34.0	2.719	0.006	2.711	0.006	2.725	0.006	2.786	0.014	2.722	0.003	0.033
9	-30.0	2.752	0.005	2.764	0.005	2.768	0.005	2.783	0.010	2.757	0.003	0.023
10	-26.2	2.780	0.004	2.802	0.004	2.793	0.003	2.809	0.007	2.792	0.003	0.019
11	-22.5	2.810	0.005	2.832	0.003	2.821	0.003	2.823	0.006	2.816	0.002	0.018
12	-18.9	2.833	0.004	2.849	0.003	2.836	0.003	2.835	0.006	2.838	0.002	0.016
13	-15.3	2.849	0.005	2.866	0.003	2.853	0.003	2.865	0.006	2.858	0.002	0.016
14	-11.9	2.872	0.006	2.884	0.003	2.868	0.004	2.892	0.007	2.877	0.002	0.018
15	- 8.5	2.884	0.005	2.896	0.003	2.886	0.005	2.889	0.006	2.886	0.003	0.018
16	- 5.1	2.902	0.005	2.905	0.006	2.894	0.006	2.923	0.010	2.906	0.004	0.025
17	- 1.7	2.889	0.013	2.895	0.004	2.884	0.006	2.916	0.010	2.894	0.003	0.024
North												
18	1.7°	2.892	0.005	2.895	0.003	2.894	0.006	2.903	0.008	2.890	0.003	0.022
19	5.1	2.898	0.005	2.900	0.003	2.881	0.004	2.921	0.010	2.888	0.003	0.022
20	8.5	2.887	0.006	2.894	0.003	2.885	0.004	2.897	0.007	2.887	0.002	0.018
21	11.9	2.867	0.005	2.885	0.002	2.867	0.004	2.878	0.004	2.874	0.002	0.014
22	15.3	2.852	0.004	2.875	0.003	2.858	0.003	2.877	0.008	2.859	0.002	0.016
23	18.9	2.837	0.004	2.856	0.003	2.845	0.003	2.849	0.005	2.841	0.002	0.016
24	22.5	2.811	0.004	2.833	0.004	2.823	0.003	2.827	0.007	2.822	0.002	0.019
25	26.2	2.790	0.004	2.816	0.004	2.821	0.006	2.806	0.006	2.803	0.003	0.021
26	30.0	2.752	0.005	2.776	0.006	2.775	0.004	2.774	0.007	2.767	0.003	0.023
27	34.0	2.709	0.007	2.736	0.008	2.729	0.006	2.793	0.012	2.730	0.003	0.031
28	38.1	2.670	0.012	2.678	0.006	2.679	0.011	2.689	0.010	2.671	0.004	0.040
29	42.6	2.632	0.012	2.633	0.012	2.627	0.010	2.649	0.014	2.619	0.005	0.046
30	47.3	2.546	0.021	2.575	0.019	2.531	0.014	2.651	0.014	2.568	0.007	0.073
31	52.6	2.464	0.014	2.445	0.018	2.501	0.018	2.591	0.017	2.498	0.008	0.096
32	58.5	2.398	0.022	2.391	0.023	2.348	0.021	2.441	0.018	2.305	0.016	0.134
33	65.8	2.250	0.030	2.279	0.034	2.310	0.025	2.392	0.022	2.242	0.020	0.137
34	72.8	2.252	0.054	2.124	0.049	2.441	0.034	2.389	0.034	2.405	0.026	0.224

TABLE 2

MAGNETIC ROTATION FOR POLAR LATITUDES AVERAGED FROM 1967 JANUARY 1 TO 1981 DECEMBER 31
BASED ON YEARLY AVERAGED CORRELATIONS

	1 Day Lag		2 Day Lag		3 Day Lag		4 Day Lag		Average over Lags		
Latitude	$\omega_l(1)$	$\sigma_l(1)$	$\omega_l(2)$	$\sigma_l(2)$	$\omega_l(3)$	$\sigma_l(3)$	$\omega_l(4)$	$\sigma_l(4)$	ω_l	σ_l	$\bar{\Delta}_l$
South:											
1 −72.8	2.174	0.045	2.210	0.057	2.202	0.069	2.095	0.038	2.172	0.026	0.056
2 −65.8	2.331	0.046	2.253	0.019	2.249	0.028	2.233	0.038	2.274	0.022	0.039
3 −58.5	2.359	0.023	2.372	0.023	2.367	0.016	2.327	0.024	2.356	0.013	0.023
4 −52.6	2.498	0.013	2.487	0.013	2.446	0.012	2.457	0.010	2.472	0.012	0.016
5 −47.3	2.568	0.009	2.560	0.007	2.531	0.008	2.597	0.006	2.564	0.016	0.015
North:											
30 47.3	2.567	0.008	2.557	0.008	2.571	0.008	2.507	0.010	2.562	0.015	0.010
31 52.6	2.485	0.010	2.486	0.014	2.477	0.013	2.454	0.012	2.478	0.009	0.014
32 58.5	2.404	0.018	2.367	0.010	2.361	0.019	2.365	0.011	2.377	0.012	0.017
33 65.8	2.272	0.032	2.220	0.024	2.253	0.026	2.244	0.023	2.249	0.019	0.029
34 72.8	2.187	0.054	2.091	0.059	2.137	0.068	2.188	0.015	2.148	0.023	0.059

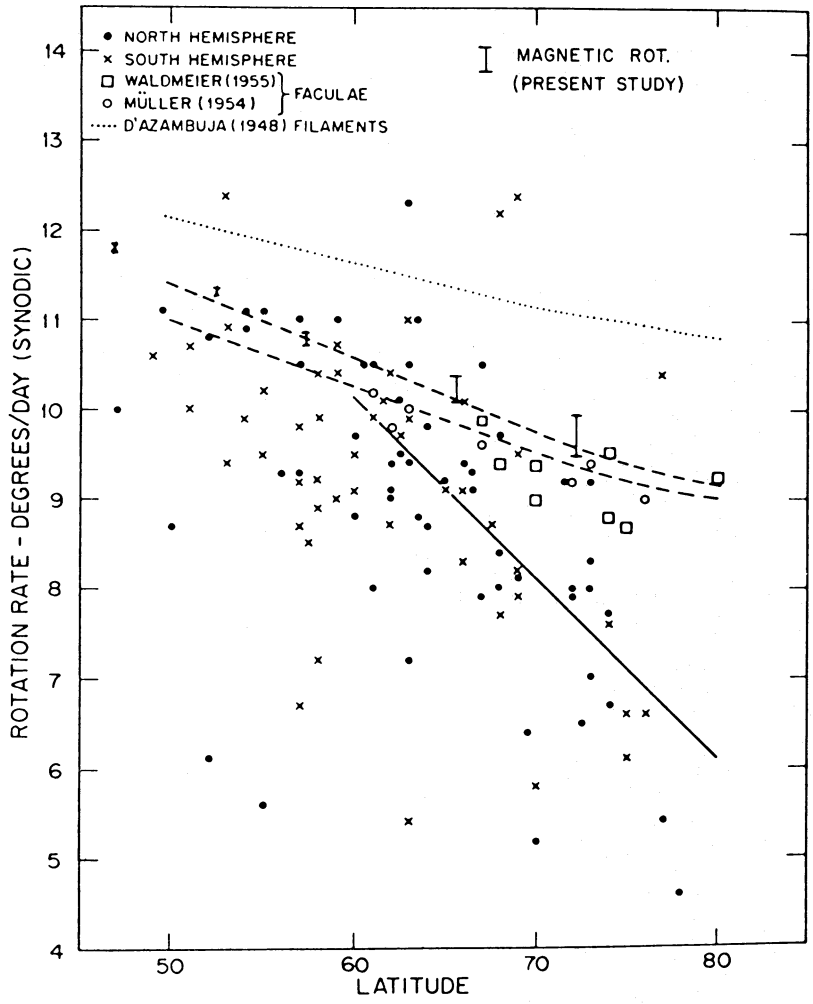

FIG. 2.—Polar magnetic rotation compared with the results of other studies. The present results are indicated by the error bars, which represent their standard deviations.

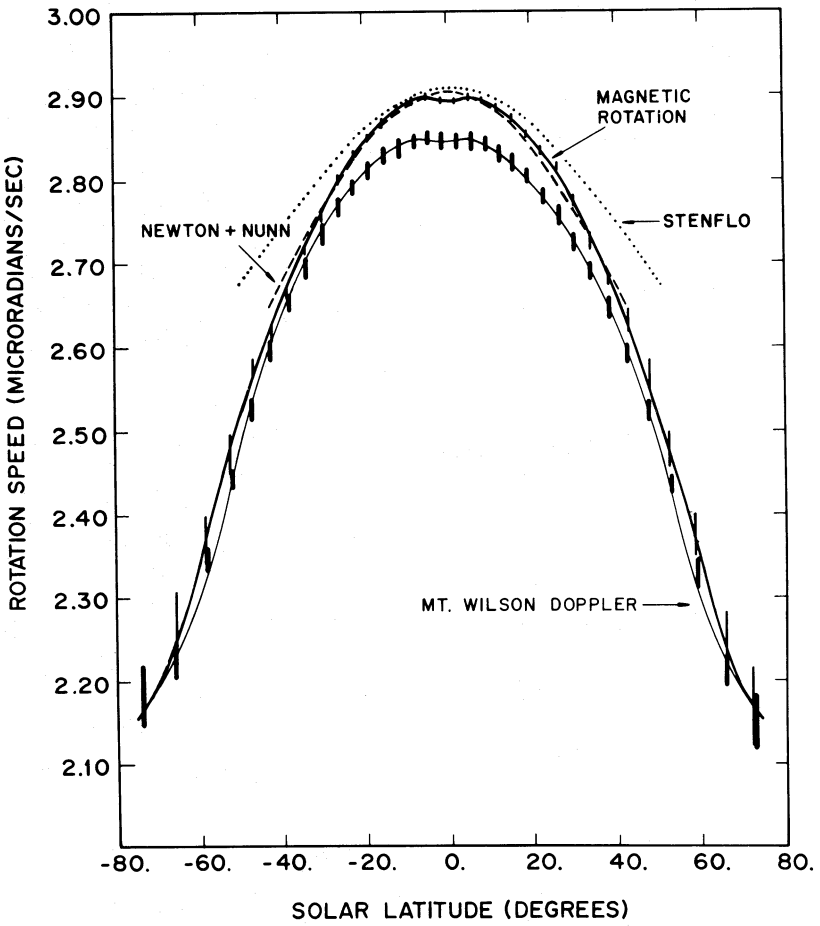

FIG. 3.—Average magnetic rotation profile for the period from 1967 January 1 to 1982 May 29. The error bars represent standard deviations. Points for latitudes less than 45° are the 2 day lag results from Table 1, and the others are the lag-averaged rates from Table 2. For comparison, the sunspot results of Newton and Nunn (1951), the magnetic rotation results of Stenflo (1974), and the Mount Wilson Doppler curve (Howard *et al.* 1983) are also shown.

of his rotation profile to imply a correlation between shear and flux density. His results are also based on Mount Wilson data, though mostly on those from the earlier period, 1959–1970, when the data were not yet fully digitized, and his bin size is considerably larger than ours.

To study such possible relationships among rates and other quantities, a number of scatter plots were made using our daily (unaveraged) results. In particular, it was found that the only effect of stronger (either average or rms) fields is to reduce the scatter in the calculated rate values. Other plots indicated that there is no correlation between the variations in rate for different latitudes, and that scatter of the calculated rate values is reduced more strongly with increased correlation sharpness than with increased correlation strength, which lends still further credence to the averaging method discussed in the Appendix.

The close agreement between our curve and that of Newton and Nunn (1951), whose results were based on observations of recurring sunspots over the six cycles from 1878 to 1944, not only supports the lack of a relationship between magnetic rate and field strength, but also argues for a long-term stability in the rate. Perhaps the most striking aspect of the results of the present study is this steadiness in the magnetic rate, which is illustrated in Figures 4*a* and 4*b* where the 2 day lag, 28 day averaged rotation rate for each latitude is exhibited as a function of time. The "error" bars are the values of Δ_t from Table 1, which provide estimates of the relative uncertainties of individual values. Symmetry between northern and southern hemispheres is evident both in mean values, which are the horizontal lines at the center of each graph, and in the scatter of points about the mean values. This scatter has been studied in some detail. In particular, it is evident that there is no general trend at any latitude toward increase or decrease in the rate over the whole time period. Individual latitudes exhibit what appears to be periodic behavior over certain intervals, but there is no

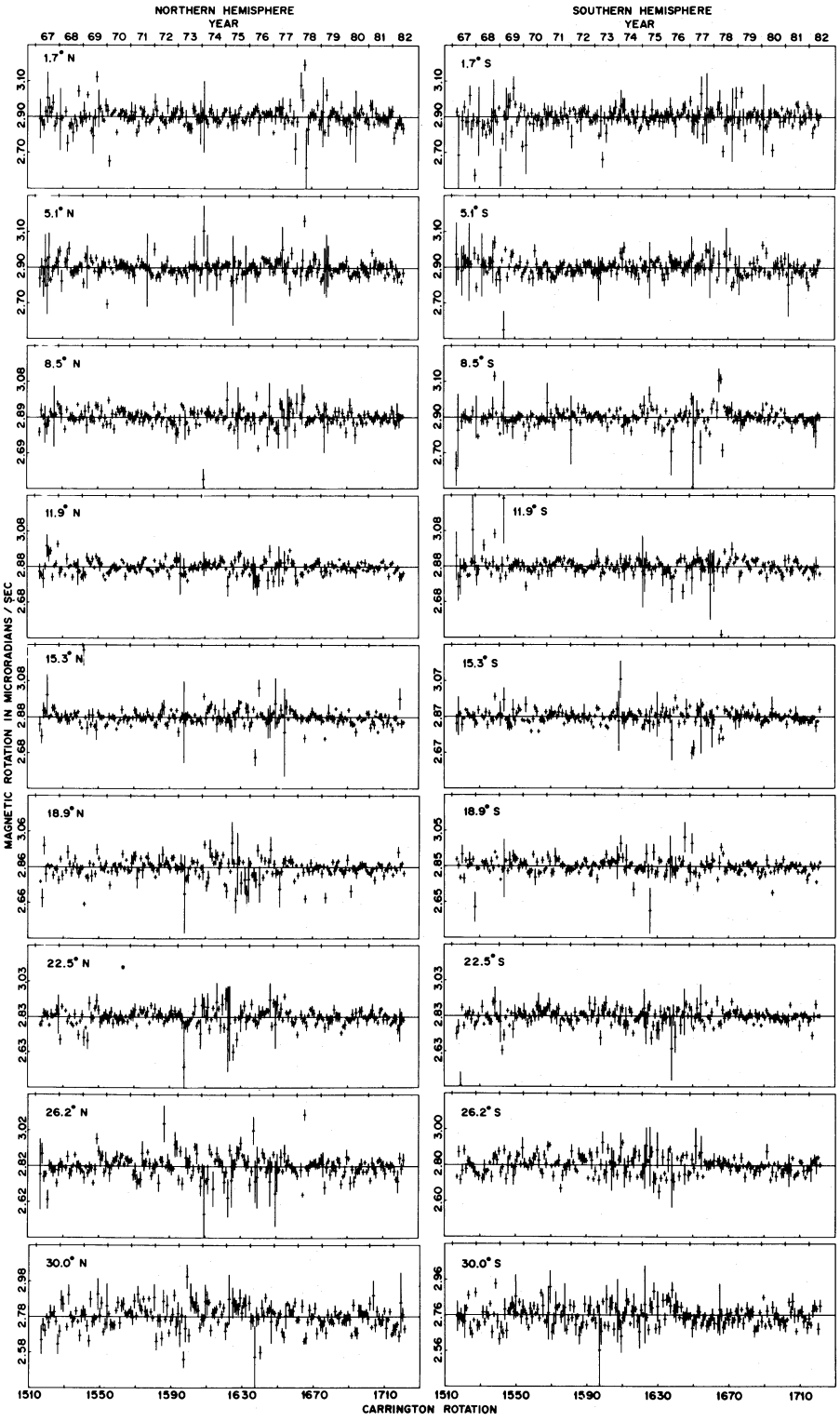

FIG. 4*a*

FIG. 4.—Magnetic rotation as a function of time calculated from cross-correlations of Mount Wilson magnetograms taken 2 days apart and averaged over perios of 28 days. The midpoint of each latitude zone is indicated on each graph, and the horizontal line at the center is the average rate from Table 1. Low-latitude ($<30°$) results are shown in Fig. 4*a* and high-latitude results in Fig. 4*b*. Note the changes in scale to accomodate the increased noise in Fig. 4*b*.

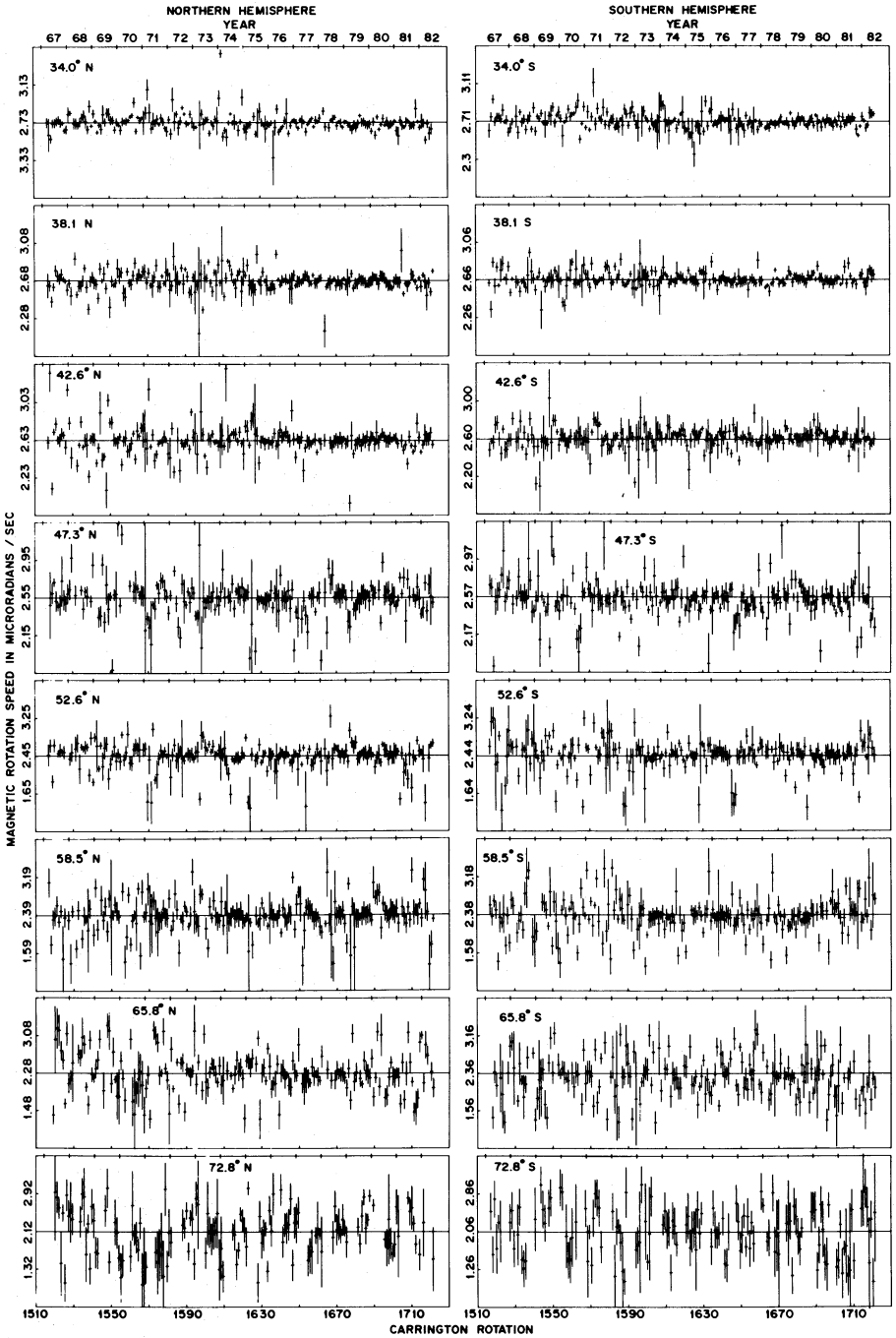

FIG. 4*b*

correspondence in this behavior between adjacent latitudes, nor do power spectra taken for each latitude show any identifiably consistent periodicities.

The scatter of individual values about the means is thus felt to be primarily random noise. It is well correlated with field strength and activity: the equatorial latitudes are noisier than those slightly higher, the best results coming from latitudes between 10° and 25°, and beyond 30° the noise increases (note the scale changes in Fig. 4*b*) steadily toward the poles where it reaches a level of roughly 35%. The gaps in these polar zones stem from the tilt of the Sun's rotation axis.

The magnetic cycle can be identified by tracing regions of greater noise, or scatter, that move upward and to the right in the sequences of the graphs in Figures 4*a* and 4*b*. These regions indicate periods of weak fields and

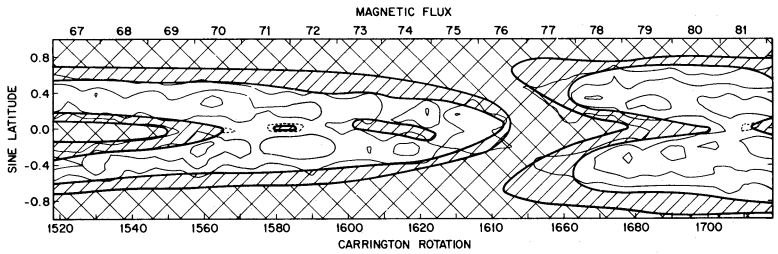

FIG. 5.—The relation of noise in the magnetic rotation calculation to magnetic activity over the cycle. The averaged magnetic flux contours are taken from Howard and LaBonte (1981, Fig. 3*a*), and the regions for three increasing levels of noise from Fig. 2 are indicated by nonhatched, single-hatched, and cross-hatched areas.

low magnetic activity: the tail of one is visible at the top left of Figure 4*a*, and another, emerging at the left center from the general noise at the top right of Figure 4*a*. The connection with the cycle is shown in Figure 5, which locates these regions on a chart of magnetic flux (Howard and LaBonte 1981, Fig. 3*a*).

Returning to Figure 3, the error bars are the standard deviation of the means for the whole period. In the Doppler case, random errors of $\sim 0.25\%$ are found for all latitude zones out to $\pm 60°$, rising to $\sim 1\%$ at the poles, and in the magnetic case, the errors are $\lesssim 0.1\%$ out to $\pm 30°$, rising to $\sim 1.1\%$ at the poles. The magnetic results thus have 2–3 times less scatter for mid to low latitudes and are of comparable precision elsewhere.

It might seem, therefore, that we should easily find the torsional oscillations in our magnetic results, if they exist with comparable amplitude to the Doppler torsional oscillations (Howard and LaBonte 1980). That they are not evident either in Figures 4*a* and 4*b* or in the power spectra may be accounted for by the difference in the nature of the noise in the two methods. The Doppler fluctuations for different latitudes are tightly correlated, so that, in relation to a daily reference rate determined at any particular latitude, the residual fluctuations over the remaining latitudes are reduced by better than an order of magnitude (LaBonte and Howard 1981*a*). It is in comparison with these residual fluctuations that the torsional oscillations stand out. In the magnetic results, the fluctuations for different latitudes are uncorrelated, and the random noise, which is considerably above the expected torsional amplitude, cannot be thus reduced. Furthermore, as is seen in § IV*a*, a systematic masking error arises in the binning of the data.

A standard means of summarizing solar rotation profiles is by fitting them with the functional form

$$\omega(\phi) = A + B \sin^2 \phi + C \sin^4 \phi \,, \qquad (1)$$

where ϕ is the solar latitude (Howard and Harvey 1970). Here A is an "absolute" rotation rate, and B and C give the "differential" rotation. In spite of nonorthogonality, this provides a convenient and good fit for the Mount Wilson Doppler results, though it cannot reproduce the equatorial dimple. The coefficient A absorbs the bulk of the scatter, and a torsional oscillation pattern can be clearly seen by plotting B and C versus time (Howard *et al.* 1983). Representation of the magnetic results in this form is not as successful. The curve is different in shape, and as would be expected from the discussion of the preceding paragraph, and the scatter in A is less while that in B and C is an order of magnitude greater. This is seen in Table 3 where the magnetic and Doppler coefficients, averaged over 1967–1981, are compared. The considerable differences among the B and C coefficients result from tradeoffs due to nonorthogonality. The Doppler A coefficient given here has been corrected (LaBonte and Howard 1981*a*) for fringes and scattered light.

IV. DISCUSSION

a) Effects of Bin Size and Number

All variances given in Table 1 and Figure 3 are rms scatter about mean values and are overly generous estimates of random noise because they presume no actual variability in the rates. Since they do not adequately account for the differences among the means, the question is whether this failing is due to systematic

TABLE 3

AVERAGED SOLAR ROTATION COEFFICIENTS AND THEIR VARIANCES FROM 1967 JANUARY 1 TO 1981 JANUARY 1

ROTATION PROFILE	COEFFICIENT		
	A	*B*	*C*
Magnetic: 2 day lag	2.902 ± 0.002	−0.464 ± 0.018	−0.328 ± 0.029
Magnetic: Average over lags	2.890 ± 0.001	−0.400 ± 0.013	−0.434 ± 0.023
Doppler	2.857 ± 0.006	−0.347 ± 0.005	−0.477 ± 0.007

errors or to real solar phenomena. The ultimate limits of accuracy are set by the drift and change of the fields between observations, and the wide scatter in the daily rates stems primarily from this condition. Thus it is not clear that a refinement in bin size would result in much reduction in the noise level. A systematic error arises, however, out of the disk projection described in § II. The uneven longitudinal lengths of the original bins cause the "flow" of features to be uneven in a way that cannot be removed by interpolation, and when combined with the correlation operation this leads to a slight but systematic lowering of the calculated rate. Numerical experiments indicate that the magnitude is close to the noise level for the 1 day lag, but less for longer lags.

A second systematic error stems from the latitude-width of the bins, i.e., the width of the latitude strips. Owing to the rotational shear, features on the low-latitude sides will outpace those on the high sides. The average rates should thus be uncertain by at least an amount comparable to the shear, as is confirmed in Figure 3 if we bear in mind that the error bars represent variances of the means. But we also get a systematic flattening of the differential rotation profile and a bogus oscillation, for the correlations are dominated by the strongest field features, which on average tend to lie on the more active side of each latitude zone, and this tends to pull the calculated speed upward for high latitudes and decrease it at the equator. The flattening should vary with the solar cycle as the sunspot latitudes drift toward the equator, resulting in a false "torsional oscillation" of sign opposite to that found by Howard and LaBonte (1980). A rough estimate of the magnitude of this effect indicates that it is comparable to the magnitude of the real torsional oscillations and so tends to mask them.

When the number of bins is small, the correlation calculation itself is inaccurate. The standard random error $\sim(n-1)^{-1/2}$ (Dodes and Greitzer 1964) is of course reduced by correlation averaging, and though the number of bins is less at higher day lags, the resulting error in rate is also less because of being divided by the time interval. On the other hand, as we begin to run out of bins, edge effects appear; as confirmed by studying the daily results, this condition is the cause of the unevenness seen in Table 1 in the 4 day rate near the equator.

More interesting is a systematic error introduced in the correlation calculation which will be discussed in detail in a separate paper, presently in preparation. Briefly, the combination of extraction of the mean with shrinkage of the correlation domain as the lag is increased produces an asymmetry in the correlation peak which causes the fit to underestimate its displacement. All calculated rates are thus slightly low, and for the bin size and number used in this project the resulting variation of rate with day lag essentially matches that seen in Table 1 for mid to low latitudes. We therefore conclude that this variation in rate with time is an alias of the calculation, and have focused on the 2 day case, where the magnitude of this error is least.

b) Comparison of Doppler and Magnetic Determinations of Solar Rotation

Although line shift and Zeeman splitting are measured together, Doppler and magnetic determinations of solar rotation have little else in common. Doppler rotation is defined (Howard, Boyden, and LaBonte 1980) by the antisymmetric part of a fitted curve of line shift versus longitude, after corrections have been subtracted for the Earth's orbit and rotation and for a standard limb redshift. Magnetic rotation is defined by the displacement of a correlation peak. Hence, even excluding the problems of measurement and calculation, one ought to be cautious in asserting that a difference in these rates means plasma and fields rotate differently.

Factors that limit the accuracy of the magnetic calculation include, in addition to the binning and correlation problems discussed above, the time interval, during which the fields change. As discussed in § III, this factor seems to be the major source of random error. The magnetic result is also sensitive to the fit chosen for the correlation peak and to the way in which all averages that are taken are weighed. On the other hand, it is unaffected by problems of calibration or instrumental drift and is free from the most pernicious systematic error sources, i.e., stray fringes and scattered light, which lower the Doppler result.

Overall, the cross-correlation determination of magnetic rotation is less problematic than the Doppler determination of plasma rotation. Except at the poles, the levels of noise are lower in the *absolute* rates (provided the correlations are averaged as described in the Appendix) and noise is uncorrelated from latitude to latitude. Though, judging from the Doppler determination of rotational shear as discussed in § III, the Doppler approach is potentially the more accurate—at least given the bin size and averaging procedure used in this project—the scatter in the absolute Doppler rate suggest that some instrumental or stray fringe effects remain as yet at large, and this at least for now gives the magnetic determination a slight edge in accuracy.

V. CONCLUSION

We have found the day-to-day rotation of solar magnetic features to be steady over the whole solar surface, showing neither measurable dependence on field strength nor variation with time. The remarkable agreement of our results with the widely accepted sunspot results of Newton and Nunn gives extra support to these findings. When compared with the presently accepted Doppler-determined plasma rate, the magnetic rate is roughly 1.5% (~ 30 m s^{-1}) faster, except near the poles. The level of precision in the magnetic results is not quite sufficient for resolving the expected torsional oscillations that are seen in the more accurately measured Doppler shear; however, our margin of error in determining the mean values for the *absolute* magnetic rate as a function of latitude is the smallest for any solar rotation study to date.

The author wishes to express deep appreciation to Dr. Robert Howard, who suggested this project and whose careful work over the past 20 odd years produced the data base that made it possible, and to thank him as well for many useful and encouraging discussions. Thanks are also owed to Dr. David Bruning for help at the beginning with the correlation and fitting routines, to John Boyden for help with the programming, and to others, including Larry Webster, Nancy Newton-Tomer, and Maria Anderson who were also of great assistance. All computations were performed on the Mount Wilson solar department's Raytheon 704 computer. Grant support came from the National Science Foundation (grant AST 80-20445), the National Aeronautics and Space Administration (grant NGR-09-140-015), and the Office of Naval Research (contract N00014-81-C-0065).

APPENDIX

THE THREE-POINT PARABOLIC FIT AND THE WEIGHTING OF CORRELATION AVERAGES

Referring to Figure 6, a three-point parabolic fit to $C_j^{j+n}(L)$ interpolates a maximum $C(L_0)$ at lag L_0, where

$$L_0 = L_B + \frac{C - A}{2[2B - (C + A)]} . \tag{A1}$$

Since the lags at which values of C_j^{j+n} are calculated are spaced at equal intervals $L = d$, the quantities $[C - A]$ and $[2B - (C + A)]$ are proportional, respectively, to the approximated slope and curvature (sharpness) at lag L_B. The calculated angular speed is

$$W_j = L_0/T_n , \tag{A2}$$

where T_n is the time interval. To average a set of speeds thus calculated, a weighting factor p_j must be chosen:

$$\bar{\omega} = \sum p_j \omega_j / \sum p_j . \tag{A3}$$

It would not seem appropriate to weight strong and weak correlations equally ($p_j \equiv 1$)—more reasonable choices might be $p_j = B$ or $p_j = C_i^{i+n}(L_0)$. Another choice would be the "sharpness" of the correlation peak, $2B - (A + C)$, which involves the same three points as are used in the fit.

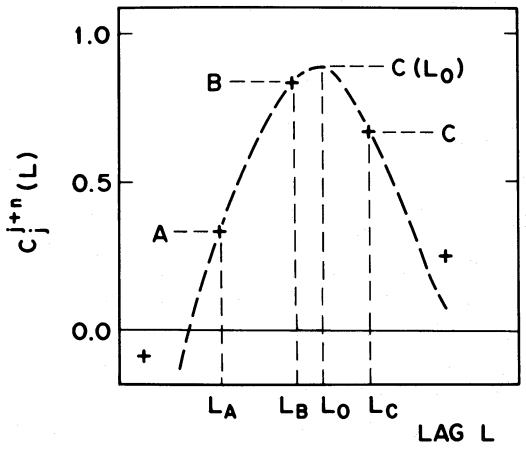

FIG. 6.—A three-point parabolic fit to locate the maximum for a correlation curve. A, B, and C represent calculated correlation values C_j^{j+n} at lags L_A, L_B, and L_C respectively. $C(L_0)$ and L_0 are the fitted maximum and its lag.

The second approach to finding the average speed, which makes fitting easier when the correlations are noisy, is to first average the correlation curves themselves:

$$C_n(L) = \frac{\sum C_j^{j+n}(L)}{\sum j} \tag{A4}$$

(here unit weight seems appropriate), having carefully adjusted the binning framework as described in § II so that the time intervals are all equal. Fitting the averaged curve now gives a rate

$$\bar{\omega} = \bar{L}_0/T . \tag{A5}$$

In general, $\bar{\omega} \neq \bar{\omega}$. However, if the correlations to be averaged peak at the same lag L_B, and if we choose sharpness as the weighting function,

$$p_j = 2B - (A + C) , \tag{A6}$$

then the denominator in equation (A1) is cancelled and the averages agree:

$$\begin{aligned} \bar{\omega} &= \frac{\sum [2B - (A + C)]L_0/T}{\sum [2B - (A + C)]} \\ &= \frac{1}{T} \frac{\sum \{(C - A)/2 + [2B - (A + C)]L_B\}}{\sum [2B - (A + C)]} \\ &= \frac{1}{T} \left\{ \frac{\bar{C} - \bar{A}}{2[2\bar{B} - (\bar{A} + \bar{C})]} + L_B \right\} = \frac{\bar{L}_0}{T} \\ &= \bar{\omega} . \end{aligned} \tag{A7}$$

When the correlations that are averaged do not all peak at the same lag, the situation is more complicated. Only those that peak at the lag where the *averaged* correlation peaks are weighted by their sharpness; the others are weighted by their curvature at this lag. Since equation (A6) is maximized when B is a maximum, correlations that do not peak where the average does get assigned artificially lowered weights. For peaks that lie close to the average (e.g., let the maximum in Figure 6 be shifted to C), this curvature remains equal to the sharpness to the extent that the curve remains parabolic (e.g., back down to A), and the conclusion of equation (A7) holds. This saves the cases where the true maxima happen to lie near the boundaries between bins. On the other hand, spurious peaks are weeded out entirely.

REFERENCES

Altschuler, M. D., Trotter, D. E., Newkirk, G., Jr., and Howard, R. 1974, *Solar Phys.*, **39**, 3.
Babcock, H. W. 1953, *Ap. J.*, **118**, 387.
Bumba, B., and Howard, R. 1965, *Ap. J.*, **141**, 1502.
Dodes, I. A., and Greitzer, S. L. 1964, *Numerical Analysis* (New Jersey: Hayden), p. 118.
Howard, R. 1974*a*, *Solar Phys.*, **38**, 59.
———. 1974*b*, *Solar Phys.*, **38**, 283.
———. 1974*c*, *Solar Phys.*, **39**, 3.
———. 1974*d*, *Solar Phys.*, **39**, 275.
———. 1976*a*, *Solar Phys.*, **47**, 576.
———. 1976*b*, *Solar Phys.*, **48**, 413.
———. 1977, *Solar Phys.*, **52**, 243.
———. 1978*a*, *Solar Phys.*, **59**, 243.
———. 1978*b*, *Rev. Geophys. Space Phys.*, **16**, 721.
Howard, R., Adkins, J. M., Boyden, J. E., Cragg, T. A., Gregory, T. S., LaBonte, B. J., Padilla, S. P., and Webster, L. 1983, *Solar Phys.*, in press.
Howard, R., Boyden, J. E., and LaBonte, B. J. 1980, *Solar Phys.*, **66**, 167.
Howard, R., and Edberg, S. 1973, *Solar Phys.*, **28**, 73.
Howard, R., and Harvey, J. 1970, *Solar Phys.*, **12**, 23.
Howard, R., and LaBonte, B. J. 1980, *Ap. J.* (*Letters*), **239**, L33.
———. 1981, *Solar Phys.*, **74**, 131.
Howard, R., and Stenflo, J. O. 1972, *Solar Phys.*, **22**, 402.
Howard, R., and Yoshimura, H. 1976, in *IAU Symposium 71, Basic Mechanisms of Solar Activity*, ed. V. Bumba and J. Klezck (Dordrecht: Reidel), p. 19.
LaBonte, B. J., and Howard, R. 1981*a*, *Solar Phys.*, **73**, 3.
———. 1981*b*, *Solar Phys.*, **75**, 161.
———. 1983, *Solar Phys.*, in press.
LaBonte, B. J., Howard, R., and Gilman, P. A. 1981, *Ap. J.*, **250**, 796.
Newton, H. W., and Nunn, M. L. 1951, *M.N.R.A.S.*, **111**, 413.
Stenflo, J. 1974, *Solar Phys.*, **36**, 495.
———. 1977, *Astr. Ap.*, **61**, 797.
Ward, F. 1965, *Ap. J.*, **141**, 534.
———. 1966, *Ap. J.*, **145**, 416.
Wilcox, J. M., and Howard, R. 1970, *Solar Phys.*, **13**, 251.
Wilcox, J. M., Schatten, K. H., Tannenbaum, A. S., and Howard, R. 1970, *Solar Phys.*, **14**, 255.

HERSCHEL SNODGRASS: Mount Wilson and Las Campanas Observatories of the Carnegie Institution of Washington, 813 Santa Barbara Street, Pasadena, CA 91101